

Predicting the geometry of channelized deep-sea turbidites

W. Brian Dade
Herbert E. Huppert

Institute of Theoretical Geophysics, Department of Earth Sciences and Department of Applied Mathematics and Theoretical Physics, University of Cambridge, Cambridge CB2 3EQ, United Kingdom

ABSTRACT

Analytical relationships between the dynamic properties of a deposit-forming turbidity current propagating across a sea floor with small slope and the geometry of the resulting deposit have been confirmed experimentally for a wide range of particle sizes, initial concentrations, and volumes of the driving suspension. These simple expressions provide a basis for inferring the dynamics of natural flows from their deposits. We surmise that the turbidity current responsible for depositing the Black Shell turbidite in the northwestern Atlantic Ocean had an initial sediment concentration on the order of 100 g of silt per litre and a volume on the order of 1000 km³.

INTRODUCTION

Suspension-driven gravity flows, or turbidity currents, are a primary mechanism by which terrigenous sediment is transported into the deep sea. A turbidity current can originate from a debris flow or gravity slide associated with sea-floor failure on the continental shelf or upper continental slope. The resulting flow can be self-sustaining and can propagate rapidly down the continental slope through a network of submarine canyons. When a turbidity current debouches onto the relatively gentle slopes of the continental rise and abyssal plain, the flow collapses under its own weight, decelerates, and ultimately "runs out" over a distance determined by the loss of the driving suspension.

Particles that settle from the suspension may contribute to the channel-and-levee complex of a lower fan or to the more extensive sedimentary veneer of a deep-sea plain. In either case the resulting turbidite is recognized in the most general terms by its lenticular geometry. The turbidite can comprise medium-to-thick beds of relatively coarse sediment (silt and fine sand vis à vis the clay-rich muds resulting from pelagic sedimentation) as well as displaced fauna transported from the shallow-water source area. In addition the deposit may exhibit a diagnostic sequence of bed forms and size grading (Pickering et al., 1989).

Considerable effort has been made to relate the gross geometry of turbidites to the geologic setting of the deep-sea basins in which they are found (e.g., Pilkey et al., 1980; Pilkey, 1987), to reconstruct the hydraulic history of deposit-forming turbidity currents (e.g., Bowen et al., 1985), and to delineate experimentally the hydraulic con-

trols of deposit thickness (e.g., Middleton and Neal, 1989). We report here simple scaling arguments, derived in detail in Dade and Huppert (1994), for the length and average thickness of a turbidite generated by a gravity current undergoing self-weight collapse on a sea floor of negligible slope. Our analytical results are confirmed by both previously and newly reported data. The scalings are applicable to deposits found in two-dimensional settings, such as in channels of the lower parts of deep-sea fans and on the floors of elongate abyssal plains and subduction trenches where ponding of a deposit-forming flow does not occur. Using these relationships, a geologist can predict the downstream extent and average thickness of a turbidite resulting from a suspension-driven flow of known properties. Alternatively, one can infer the properties of the flow that generated a given deposit.

BASIS FOR THE RUN-OUT BEHAVIOR OF TURBIDITY CURRENTS IN THE DEEP SEA

Bonnecaze et al. (1993) obtained numerical solutions to the coupled partial differential equations that describe the conservation of total mass, suspended sediment, and momentum of a suspension-driven gravity flow on a horizontal surface. An important dimensionless ratio used in describing the behavior of such a flow is the Froude number, Fr , defined by

$$Fr = u/(g'h)^{1/2}, \quad (1)$$

where u is the flow speed, $g' = g\phi\Delta\rho_s/\rho$ is the reduced gravity of the driving suspension in terms of the volumetric concentration ϕ and relative excess density $\Delta\rho_s/\rho$ of the suspended particles, and h is the depth of

the flow. On gentle slopes Fr is close to unity. By using a well-established, depth-dependent relationship for values of the Froude number existing at the current head (Huppert and Simpson, 1980), Bonnecaze et al. (1993) achieved considerable success in predicting numerically the run-out behavior and the resulting deposits of suspension-driven flows generated in the laboratory.

The analysis of Bonnecaze et al. (1993) is based on the understanding that the gravity flows are turbulent. Additionally, the fine particles in suspension, such as fine sands and silts, must satisfy the condition

$$w_s \ll (g_o'h_o)^{1/2}, \quad (2)$$

where w_s is the average settling velocity of the particles in still water, and the subscript o indicates initial values. The right-hand side of equation 2 represents a velocity scale u_o for the current as it enters the depositional basin. Equation 2 is thus equivalent to the condition $w_s \ll u_o$ and, accordingly, suspended particles can be assumed to be well mixed throughout the turbulent flow (Middleton and Southard, 1984).

To make the results of the analysis by Bonnecaze et al. (1993) more accessible for geological applications, we have developed a simplified scheme that yields analytical approximations for the run-out behavior of a turbidity current on a gentle slope (Dade and Huppert, 1994). Our approach represents an extension of the simple box model developed by Huppert and Simpson (1980) for an analogous saline or nondepositing flow. Our model includes the effects of the slow settling of suspended sediments satisfying equation 2. In this model a two-dimensional gravity current is treated as a series of equal-

TABLE 1. LENGTH AND TIME SCALES FOR THE ANALYSIS OF DEEP-SEA TURBIDITES

Characteristic deposit thickness (δ)	Run-out distance (x_r)	Run-out time (t_r)
$1/3(\phi_o/\phi_b)(q_o^2 w_s^2/g_o')^{1/5}$	$3(g_o' q_o^3/w_s^2)^{1/5}$	$\gg 2(q_o^2/g_o' w_s^3)^{1/5}$

Note: ϕ_o is the initial concentration of solids suspended in the flow; $\phi_b \approx 0.5$ is the concentration of sediment in the bed; $g_o' = g\phi_o\Delta\rho_s/\rho$ is the reduced gravity of the initial suspension, where g is the acceleration due to gravity and $\Delta\rho_s$ is the excess density of particles in a fluid of density ρ ; q_o is the initial volume per unit width of the flow; and w_s is the average settling velocity of the particles in the suspension.

area rectangles that collapse under their own weight and propagate across the sea floor. Although mathematically less rigorous than the approach of Bonnezaze et al. (1993), our analysis provides explicit equations for the current speed, height, and deposit thickness as functions of time or propagation distance. These expressions can be readily applied to the study of suspension-driven gravity flows occurring either in nature or in the laboratory.

Among the potentially powerful results of our approach are explicit relationships between the length and average thickness of a turbidite and the initial properties of the deposit-forming flow. These relationships are summarized in Table 1 for deep-water turbidity currents. The run-out distance x_r , achieved over the time t_r , corresponds to the approximate limit of surge propagation due to deposition of the driving suspension. The characteristic thickness of a deposit δ is simply the thickness expected if the total mass of sediment in the initial suspension were spread uniformly over x_r .

Unlike turbidity currents in the deep sea, most experiments are conducted under conditions in which the height of the gravity current is a significant fraction of the overall depth of the host channel. Under these conditions a return flow is generated, and a description of the propagation of the surge is more complicated. The relevant expressions for these shallow-water currents are subtly different from those given in Table 1 (see Dade and Huppert, 1994). The difference between the deep- and shallow-water regimes arises primarily from the depth-dependent Froude number of the current head. Under either deep- or shallow-water conditions, however, the run-out distance of a suspension-driven surge varies directly with the initial excess density and volume of the current and inversely with the average settling velocity of the particles in the driving suspension. Alternatively, the average thickness of a deposit is proportional to the total volume of the current and to the initial con-

centration and settling velocity of the particles in suspension.

We conducted laboratory experiments to validate the shallow-water relationships linking the length and thickness of a deposit to the initial properties of the suspension-driven flow. Individual gravity flows were generated by the release of a specified volume of water laden with silicon carbide grit of various grain sizes into a horizontal channel of clear, still water. The intruding fluid was denser than the clear water and so flowed along the smooth channel floor. The particles in suspension had a specific gravity of 3.217 and diameters between 23 and 53 μm . Further details of flume geometries and experimental conditions can be found in either Bonnezaze et al. (1993) or Dade and Huppert (1994).

In one set of experiments (series A), the particle deposit resulting from each flow was first measured as a function of distance downstream from the point of release. An estimate of the length \hat{x}_r of the resulting deposit (where experimental observations are denoted by a caret) was then made by graphically extrapolating to zero thickness the measurements most distant from the flow origin. In a second set of experiments (series B), \hat{x}_r was obtained in real time by noting visually the approximate distance at which the particle deposit began to thin rapidly as it was being laid down. This method afforded an easily obtained but subjective underestimate of the run-out distance that was nevertheless found to be well correlated with the more direct estimates of series A. For each series, we derived a measure of the average areal density of the deposit over the run-out length. This measure is defined as $\eta = \rho_s \phi_o q_o / x_r$, the average mass deposited per unit of area of the channel floor, where ρ_s is the density of individual particles, ϕ_o is the initial concentration of particles in suspension, and q_o is the initial volume per unit width of the suspension. The relationship between average thickness δ and η is then given by $\eta = \rho_s \phi_b \delta$, where ϕ_b is the volu-

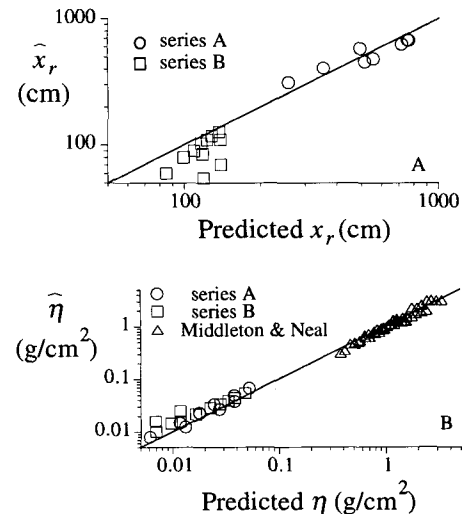


Figure 1. Comparison of predicted and observed geometries of deposits from suspension-driven gravity currents generated in the laboratory. Solid lines indicate 1:1 correspondence, and observed quantities are denoted by caret. A: Run-out distance or deposit length x_r . B: Average mass deposited per area of channel floor η . Data of Middleton and Neal (1989) expressed in terms of η calculated from their reported values of characteristic bed thickness and $\phi_b = 0.5$.

metric concentration of sediment in the bed and typically has a value of ~ 0.5 .

Comparisons of our experimental estimates and the shallow-water box-model approximations for the run-out distance and the characteristic thickness of deposit appear in Figure 1. These comparisons are presented on logarithmic axes to accommodate the full range of the available data. We report estimates of both the deposit length or run-out distance \hat{x}_r and the deposit thickness in terms of $\hat{\eta}$, but emphasize that for deposit-forming currents of constant volume the two estimates are interdependent. We also include comparisons of our box-model approximations with estimates, previously reported by Middleton and Neal (1989), of deposit thickness resulting from densely concentrated, suspension-driven gravity flows of glass and plastic beads with still-water settling velocities corresponding to those of fine-to-medium sands. Conversion of thickness δ to mass deposited per unit area η was obtained with the relationship defined in the previous paragraph and $\phi_b = 0.5$.

In general, the agreement between predicted and observed geometries of laboratory-generated deposits is good. In the case of the data of Middleton and Neal (1989), the measurements were made for dense mixtures ($0.2 \leq \phi_o \leq 0.4$) in which hindered settling would have reduced the effective

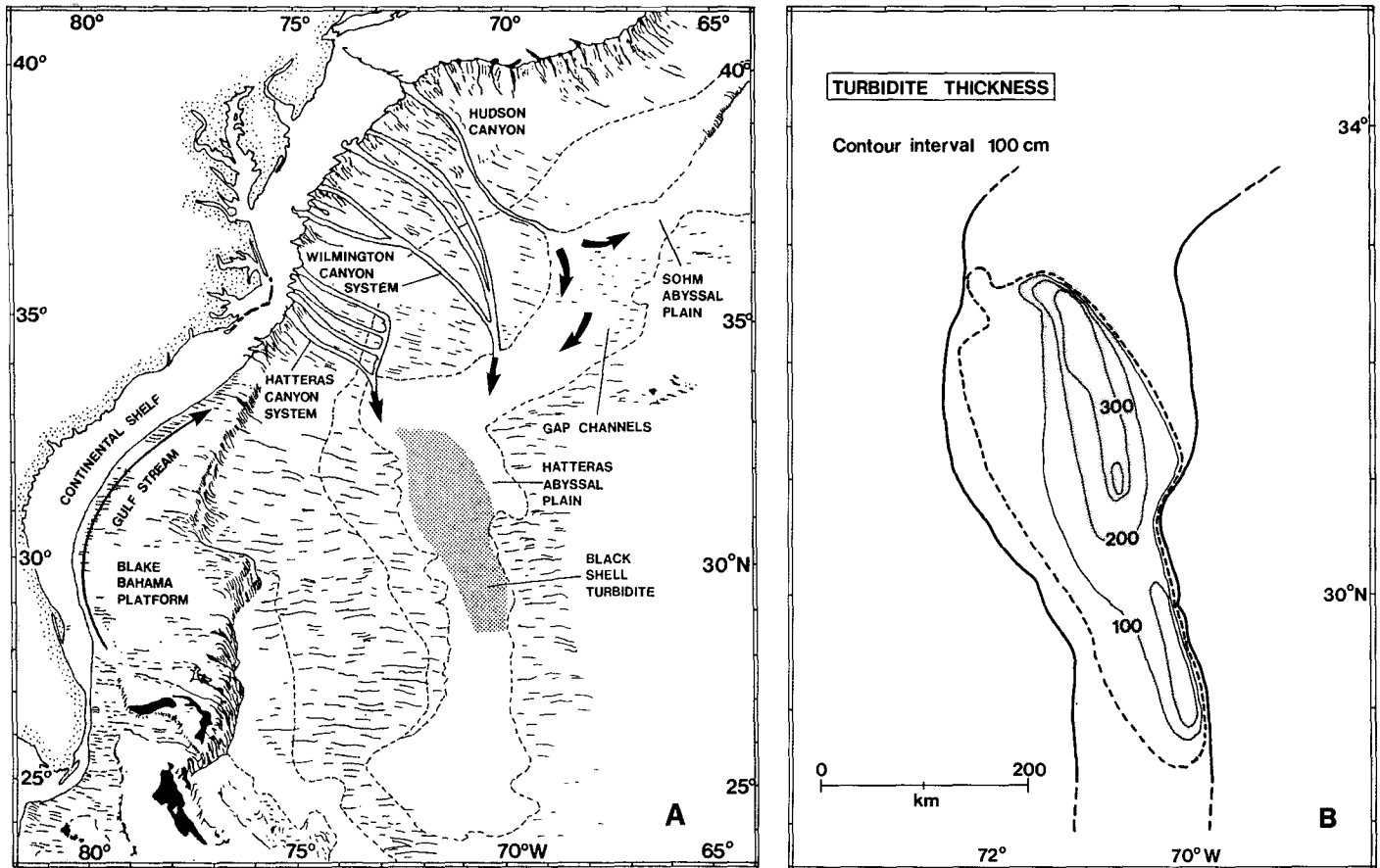


Figure 2. A: Hatteras Plain. Arrows indicate main routes of sediment supply from Hatteras Canyon system. Shaded area indicates distribution of Black Shell turbidite. B: Isopach map of Black Shell turbidite. Shaded region indicates central swath for which estimated range of deposit thickness is depicted in Figure 3. Redrawn from Elmore et al. (1979) and Pickering et al. (1989).

settling velocity of the particles in suspension at early times. Nevertheless, the good agreement shown in Figure 1 between predicted and observed geometries of the deposits laid down by suspension-driven gravity flows confirms our box model approximations over a wide range of particle sizes (medium silt to medium sand) and initial concentrations of suspended sediment ($0.01 \leq \phi_0 \leq 0.4$, corresponding approximately to $10\text{--}1000 \text{ kg/m}^3$ in the case of particles with the density of quartz).

APPLICATION TO THE GEOLOGIC RECORD

We emphasize that the expressions in Table 1 apply quantitatively only to phenomena occurring in deep-water channels and elongate basins in which the slope of the bed is small and the deposit-forming flows are laterally constrained. Reentrainment of newly deposited material is not included in the model from which these scaling relationships are derived, and, consequently, local, syndepositional reworking of a deposit is not considered. We are encouraged by the good agreement between theory and experimen-

tal observations, however, to propose that the analytical relationships given in Table 1 can be applied to geophysical phenomena in the broadest terms.

Successful correlations of horizontally extensive turbidites are rare. The Pleistocene-age "Black Shell turbidite," found on the Hatteras Plain and described by Elmore et al. (1979), appears to be among the most voluminous turbidites that have been traced continuously in any environment. The host basin for the deposit is an elongate plain located off the eastern margin of North America (Fig. 2). The basin lies below water depths of 5.1–5.5 km and extends mainly north-south for more than 1000 km. The width of the basin is ~150–300 km and is well defined by the Blake-Bahama Outer Ridge to the west and a range of abyssal hills to the east. The sea floor has a gradient of $1/3000$, sloping to the south. The basin fill is composed primarily of sand- and silt-rich turbidites derived from the source canyons to the north (Cleary et al., 1977; Pilkey et al., 1980; Pilkey, 1987).

Among these basin-filling turbidites, the Black Shell turbidite has been traced in 35

cores over an area of $44 \times 10^3 \text{ km}^2$. It extends southward across the abyssal plain for $>500 \text{ km}$, and is $>4 \text{ m}$ thick $\sim 200 \text{ km}$ downstream from the point of initial deposition (Fig. 2). The turbidite conforms to the elongate geometry of the basin, indicating that the deposit-forming flow was essentially two-dimensional. The deposit is vertically graded, with a sand base and a mud cap, and exhibits an overall average grain size corresponding to silt-rich mud. Both Middleton and Neal (1989) and Dade and Huppert (1994) have shown that the run-out behavior of the current is relatively independent of the spread in sediment grain sizes in the driving suspension.

Our box model allows us to suggest a plausible scenario for the deep-sea turbidity current that generated this impressive deposit. Shown in Figure 3 is an estimate, obtained from the isopach map of Figure 2, of the approximate range of deposit thickness observed in a central swath of the Black Shell turbidite as a function of downstream distance. Also shown in Figure 3 are calculations from our box model (Dade and Huppert, 1994) for deposit thickness based on:

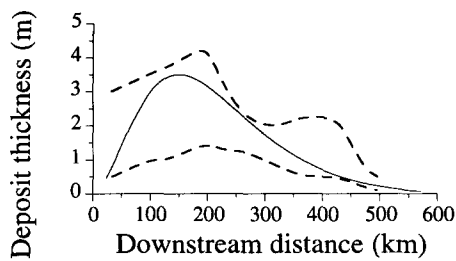


Figure 3. Thickness of Black Shell turbidite as function of downstream distance from point at which deposition began. Dashed lines represent approximate range of observed thickness in central swath shown in Figure 2B. Solid line shows calculations from box model of Dade and Huppert (1994) with parameter values given in text.

$w_s = 0.08$ cm/s (corresponding to silt-sized particles with an average diameter of 32 μ m), initial surge height and length 300 m and 30 km, respectively ($q_o = 9$ km², or equivalently a volume somewhat in excess of 1000 km³ for a basin that is 150–300 km wide), $\phi_o = 0.05$ (corresponding to ~ 130 kg/m³), and $\phi_b = 0.5$.

The model calculations capture reasonably well the lenticular geometry of the deposit, including the maximum in the observed deposit thickness at 150–200 km from the point of entry onto the plain and the onset of deposition. There are other combinations of surge properties that could have resulted in a deposit geometry similar to that delineated in Figure 3, but this combination seems likely, given the overall silty texture of the deposit. Given the suspension properties inferred from the deposit by using our model, we note from equation 1 that the initial speed of the Black Shell current as it entered the Hatteras Plain from the north would have been >10 m/s. This value is comparable with the peak flow speeds inferred from the sequence of cable breaks associated with the Grand Banks turbidity current of 1929 (Heezen and Ewing, 1952). We note, however, that the Black Shell current only marginally met the criterion for auto-suspension given by

$$w_s/|u| \ll \sin\theta, \quad (3)$$

where θ is the angle of the seafloor slope (Pantin, 1979; Parker et al., 1986). The current thus decelerated rapidly and lost its ability to transport the initial load due to the energetic demands of maintaining the turbulent suspension. Deposition, in other words, proceeded from the relatively fast but decelerating flow. The thickness maximum may be due to reentrainment and deposit reworking by the fast current at early times, or, as in our box model, it may be due simply to the limited duration of passage of the initially

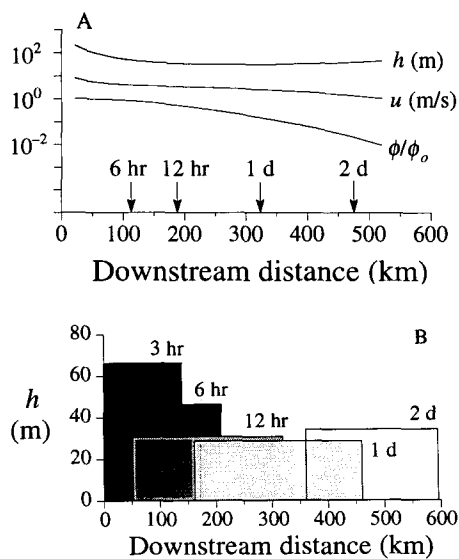


Figure 4. Reconstruction of Black Shell turbidity current using box model of Dade and Huppert (1994) and parameter values given in text. A: Average thickness h , speed u , and relative sediment concentration ϕ/ϕ_o of flow as functions of downstream distance and time. B: Box-model geometry of current as function of downstream distance and time (hours and days). Shading in each box represents progressive decrease in concentration of suspended particles.

fast current over the bed relative to the rate of deposition from the driving suspension.

We can apply the values for w_s , q_o , ϕ_o , and ϕ_b specified above in a detailed reconstruction of the Black Shell turbidity current from the point of initial deposition by using our box model (Dade and Huppert, 1994). Calculations of average speed, thickness, and relative concentration of the deposit-forming flow are shown in Figure 4. Returning to the relationships given in Table 1, we can surmise in more general terms that such a flow would have propagated >700 km downstream from the point of initial deposition and generated a deposit over this distance with an average thickness of 1 m. The depositional event would have taken place over a period of about two days.

Our expressions that relate the properties of deposit-forming gravity currents and the geometry of some deep-sea turbidites can provide a mechanistic link between dynamic events and the resulting sedimentary record. Such a link enhances both the predictability of depositional systems that have economic potential and an understanding of catastrophic sediment-transport events that occur on basin-wide scales.

ACKNOWLEDGMENTS

We thank R. C. Kerr, J. R. Lister, I. N. McCave, H. M. Pantin, R. J. S. Sparks, and J. S. Turner for helpful comments on an earlier version

of the text. M. Hallworth and M. Elliott conducted some of the experiments and drafted some of the figures. Supported in part by the Natural Environmental Research Council.

REFERENCES CITED

- Bonnecaze, R. T., Huppert, H. E., and Lister, J. R., 1993, Particle-driven gravity currents: *Journal of Fluid Mechanics*, v. 250, p. 339–369.
- Bowen, A. J., Normark, W. R., and Piper, D. J. W., 1985, Modelling of turbidity currents on Navy Submarine Fan, California Continental Borderland: *Sedimentology*, v. 31, p. 169–185.
- Cleary, W. J., Pilkey, O. H., and Ayers, A. M., 1977, Morphology and sediments of three ocean basin entry points, Hatteras Abyssal Plain: *Journal of Sedimentary Petrology*, v. 47, p. 1157–1170.
- Dade, W. B., and Huppert, H. E., 1994, A box model for non-entraining, suspension-driven gravity surge on horizontal surfaces: *Sedimentology* (in press).
- Elmore, R. D., Pilkey, O. H., Cleary, W. J., and Curran, H. A., 1979, Black Shell turbidite, Hatteras Abyssal Plain, western Atlantic Ocean: *Geological Society of America Bulletin*, v. 90, p. 1165–1176.
- Heezen, B. C., and Ewing, M., 1952, Turbidity currents and submarine slumps and the 1929 Grand Banks earthquake: *American Journal of Science*, v. 250, p. 849–873.
- Huppert, H. E., and Simpson, J. E., 1980, The slumping of gravity currents: *Journal of Fluid Mechanics*, v. 99, p. 785–799.
- Middleton, G. V., and Neal, W. J., 1989, Experiments on the thickness of beds deposited by turbidity currents: *Journal of Sedimentary Petrology*, v. 59, p. 297–307.
- Middleton, G. V., and Southard, J. B., 1984, Mechanics of sediment movement: *Society of Economic Paleontologists and Mineralogists Short Course no. 3*, 401 p.
- Pantin, H. M., 1979, Interaction between velocity and effective density in turbidity flow: Phase plane analysis, with criteria for autosuspension: *Marine Geology*, v. 31, p. 59–99.
- Parker, G., Fukushima, Y., and Pantin, H. M., 1986, Self-accelerating turbidity currents: *Journal of Fluid Mechanics*, v. 171, p. 145–181.
- Pickering, K. T., Hiscott, R. N., and Hein, F. J., 1989, Deep marine environments: London, Unwin Hyman, 416 p.
- Pilkey, O. H., 1987, Sedimentology of basin plains, in Weaver, P. P. E., and Thomson, J., eds., *Geology and geochemistry of abyssal plains*: Geological Society of London Special Publication 31, p. 1–12.
- Pilkey, O. H., Locker, S. D., and Cleary, W. J., 1980, Comparison of sand layer geometry on flat floors of ten modern depositional basins: *American Association of Petroleum Geologists Bulletin*, v. 64, p. 841–856.

Manuscript received February 7, 1994

Revised manuscript received April 22, 1994

Manuscript accepted April 27, 1994